

## SWASH ZONE MORPHODYNAMIC MODELLING INCLUDING SEDIMENT ENTRAINMENT BY BORE-GENERATED TURBULENCE

Fangfang Zhu<sup>1</sup> and Nicholas Dodd<sup>2</sup>

### Abstract

This paper investigates the effects of bore-generated turbulence on sediment entrainment in a single swash event and therefore the beachface evolution. We augment the model developed by Zhu and Dodd (2015), which includes bed- and suspended load transport, with a term specifically representing sediment entrainment at a bore (shock). The Hibberd and Peregrine (1979) swash event, which describes a uniform bore approaching the shore, is simulated. The results show that the incoming bore entrains a substantial amount of sediment into water column, and is transported in the uprush. This contributes to the relatively greater deposition in the uprush. The backwash bore generated turbulence is much smaller than that of the incoming bore, and therefore has less effect on the bed change.

**Key words:** swash, bore turbulence, sediment entrainment, beach change

### 1. Introduction

The swash zone is a very dynamic region in which the beachface is repeatedly submerged and then dried, and in which considerable sediment is also transported, as both bed and suspended load. On steeper beaches, waves collapse forming incoming bores and backwash bores (Hibberd and Peregrine 1979; Zhu et al. 2012; Zhu and Dodd 2015). There must be energy loss across the bore front (Stoker 1957), which causes vorticity and turbulence.

Bore turbulence has been recognised as being important for sediment suspension by many researchers (Jackson et al. 2004; Butt et al. 2004; Alsina et al. 2009), and particularly in the early stages of uprush. The field measurements carried out by Butt et al. (2004) show that the high suspended sediment concentration and high turbulent kinetic energy values were associated with the bore front where the near-bed flow undergoes rapid onshore acceleration. The correlation tests suggested a significant effect of turbulent kinetic energy on sediment transport across the bore, and the inclusion of bore turbulence improved significantly the sediment transport model results.

The usual approach to simulating hydro- and morphodynamics is to use a Nonlinear Shallow Water Equation description (e.g., Kelly and Dodd 2010). Sediment suspended at the bore front has been included in some modelling approaches (Kobayashi and Johnson 2001; Alsina et al. 2009) with some success. In both approaches it was assumed that energy dissipation was translated into sediment stirring, and that the turbulent kinetic energy was related to local wave energy dissipation rate. These approaches make use of algebraic or differential equations to represent turbulence production at the bore.

In this paper, we take a different approach to estimate the bore turbulence. We assume the bore turbulence is proportional to the energy loss across a shock. In order to investigate the effect of bore turbulence, we choose the swash event described by Hibberd and Peregrine (1979) (hereinafter HP79) to look at, which is a uniform bore approaching a sloping beach. We focus on the effect of bore turbulence on the suspended sediment concentration and swash zone bed evolution.

In § 2 we present the model equations. We then simulate the HP79 event to examine bore turbulence in § 3. In § 4, we draw our conclusions.

---

<sup>1</sup>Department of Civil Engineering, The University of Nottingham Ningbo China. [Fangfang.zhu@nottingham.edu.cn](mailto:Fangfang.zhu@nottingham.edu.cn)

<sup>2</sup> Faculty of Engineering, The University of Nottingham, University Park, Nottingham, UK.  
[Nicholas.Dodd@nottingham.ac.uk](mailto:Nicholas.Dodd@nottingham.ac.uk)

## 2. Model development

We augment the NSW model by Zhu and Dodd (2015), which includes bed- and suspended load transport and sedimentation / erosion, with a term specifically representing sediment entrainment at a bore (shock). The sediment entrainment due to energy loss across a bore occurs only at the bore, and this is achieved by utilising a Dirac delta function. Thus, the dimensional governing equations are

$$\hat{h}_{\hat{t}} + (\hat{h}\hat{u})_{\hat{x}} = 0, \quad (1)$$

$$\hat{u}_{\hat{t}} + \hat{u}\hat{u}_{\hat{x}} + \hat{h}_{\hat{x}} + \hat{B}_{\hat{x}} = -\frac{c_d|\hat{u}|\hat{u}}{\hat{h}}, \quad (2)$$

$$\hat{B}_{\hat{t}} + \xi\hat{q}_{\hat{x}} = \xi(\hat{D} - \hat{E}) - \xi\hat{G}(\hat{x})\delta(\hat{x} - \hat{\zeta}), \quad (3)$$

$$(\hat{h}\hat{c})_{\hat{t}} + (\hat{h}\hat{u}\hat{c})_{\hat{x}} = -(\hat{D} - \hat{E}) + \hat{G}(\hat{x})\delta(\hat{x} - \hat{\zeta}), \quad (4)$$

where  $\hat{x}$  represents cross-shore distance (m),  $\hat{t}$  is time (s),  $\hat{h}$  represents the water depth (m),  $\hat{u}$  is a depth averaged horizontal velocity ( $\text{ms}^{-1}$ ),  $\hat{B}$  is the bed level (m),  $g$  is the acceleration due to gravity ( $\text{ms}^{-2}$ ) and  $c_d$  is a dimensionless drag coefficient.  $\hat{q}$  is sediment flux due to bed load ( $\text{m}^2\text{s}^{-1}$ ),  $\hat{D}$  is the dimensional deposition rate ( $\text{ms}^{-1}$ ) and  $\hat{E}$  is the dimensional erosion (or entrainment) rate ( $\text{ms}^{-1}$ ). Here,  $\xi = 1/(1-p)$ , where  $p$  is the bed porosity.  $\hat{G}(\hat{x}) = -\hat{k}\frac{d\hat{E}}{d\hat{t}}$  and  $\hat{G}(\hat{x}) \geq 0$ , which represents the entrainment of sediment at a shock by turbulence.  $\hat{k}$  is a dimensional parameter.  $c_d$  is a dimensionless drag coefficient.  $\hat{\zeta}$  (m) is shock position. The calculation of  $\frac{d\hat{E}}{d\hat{t}}$  across a morphodynamic shock is detailed in Zhu (2012).

In figure 1 we illustrate the situation that is considered.

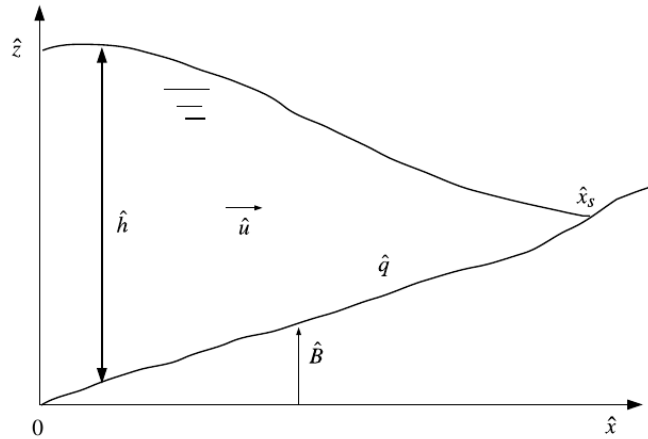


Figure1. Schematic diagram for a swash event.

We use the following forms for  $\hat{q}$ ,  $\hat{E}$  and  $\hat{D}$  (Zhu and Dodd 2015):

$$\hat{q} = \hat{A} \left( \frac{\hat{u}^2}{\hat{u}_0^2} \right)^{3/2} \frac{|\hat{u}|}{\hat{u}},$$

$$\hat{E} = \hat{m}_e \frac{\hat{u}^2}{\hat{u}_0^2},$$

$$\hat{D} = \hat{w}_s \hat{c},$$

where  $\hat{A}$  is dimensional bed-load sediment transport rate ( $\text{m}^2\text{s}^{-1}$ ),  $\hat{m}_e$  is the parameter of the sediment entrainment rate ( $\text{ms}^{-1}$ ) of suspended load,  $\hat{w}_s$  is the effective settling velocity of suspended sediment ( $\text{ms}^{-1}$ ), and  $\hat{u}_0$  is a representative velocity scale.

Therefore, equations (2.3) and (2.4) become

$$\hat{B}_t + 3\xi \frac{\hat{A}}{\hat{u}_0^3} \hat{u}^2 \hat{u}_x = \xi \left( \hat{w}_s \hat{c} - \hat{m}_e \frac{\hat{u}^2}{\hat{u}_0^2} \right) - \xi \hat{G}(\hat{x}) \delta(\hat{x} - \hat{x}_s), \quad (5)$$

$$(\hat{h}\hat{c})_t + (\hat{h}\hat{u}\hat{c})_x = - \left( \hat{m}_e \frac{\hat{u}^2}{\hat{u}_0^2} - \hat{w}_s \hat{c} \right) + \hat{G}(\hat{x}) \delta(\hat{x} - \hat{x}_s), \quad (6)$$

We follow the non-dimensionalisation in Zhu and Dodd (2015). The non-dimensional variables are

$$x = \frac{\hat{x}}{\hat{h}_0}, t = \frac{\hat{t}}{\hat{h}_0^{1/2} g^{-1/2}}, h = \frac{\hat{h}}{\hat{h}_0}, u = \frac{\hat{u}}{\hat{u}_0}, B = \frac{\hat{B}}{\hat{h}_0}, c = \frac{\hat{c}}{\hat{c}_0} \text{ and } k = \frac{\hat{k}}{\hat{k}_0},$$

where  $\hat{h}_0$  is a length scale,  $\hat{c}_0 = \frac{\hat{m}_e}{\hat{w}_s}$  is a reference concentration and  $\hat{u}_0 = (g\hat{h}_0)^{1/2}$ .  $\hat{k}_0$  is selected so that

$$\frac{1}{(g\hat{h}_0)^{1/2}} \hat{k} \frac{d\hat{E}}{d\hat{t}} = k \frac{dE}{dt}.$$

The governing equations are solved by the specified time interval method of characteristics (STI MOC) simultaneously.

### 3. Swash simulation

We investigate the swash event of a uniform bore approaching a sloping beach, which was described by the swash event of Hibberd and Peregrine (1979); the effects of bore turbulence are clearly illustrated using this case. We focus on an individual bore to see effect of bore turbulence on sediment suspension and thus beach evolution.

#### 3.1. Initial conditions

The initial conditions of a HP79 swash event are shown in figure 2. The uniform bore is in the region of  $x \leq -10$  where the bed is flat, while for  $x \geq -10$  the beach is of a uniform slope, with the beach slope  $\alpha = 0.1$ . At  $t = 0$ , there is a bore of height 0.6 propagating towards the beach and located at  $x = -10$ ; there is therefore a discontinuity in  $h, u$  and  $B$  at  $x = -10$ , separating left ( $L$ ) and right ( $R$ ) regions. For  $x \geq -10$ ,  $h(x) = 1 - \alpha(x + 10)$ ,  $u(x) = 0$ ,  $B(x) = \alpha(x + 10)$  and  $c(x) = 0$ . For  $x \leq -10$ ,  $h(x) = h_R$ ,  $u(x) = u_R$ , and  $B(x) = B_R$ . For the suspended sediment in the  $x \leq -10$  region, we assume it is steady state and therefore  $c(x) = u_R^2$ .

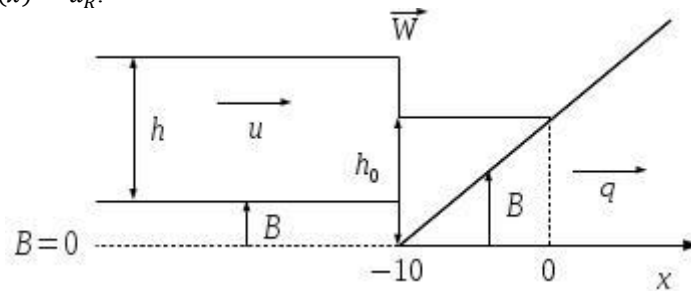


Figure 2. The initial conditions of a HP79 swash event.

#### 3.2. Simulation results

The inclusion of bore turbulence is indicated by the  $k$  value. When  $k = 0$ , it means that there is no sediment entrainment due to bore turbulence. When  $k$  increases, the process of sediment suspension by bore turbulence is assumed to be activated and progressively enhanced. The HP79 swash is simulated using the model developed to examine the effect of bore turbulence. The contour plots for different  $k$  values ( $\sigma = 0.01, M = 0.001, \tilde{E} = 0.01, c_d = 0.01$ ) are shown in figure 3.

The uniform bore approaches the shore, and collapses at  $x = 0$  at  $t = 7.47$ , causing a large amount of

sediment entrainment. The water runs up the beach and reaches the maximum run-up  $x \approx 18$  at  $t \approx 35$ . The shoreline remains static during the backwash (Zhu and Dodd, 2013), but we can see that the water moves seawards leaving a very thin film of water in the upper swash (figure 3 (a)-(b)). The backwash flow is slow due to the existence of bed shear stress and the continuous incoming flow, and the suspended sediment concentration is generally low. A backwash bore develops in simulations with all  $k$  values, and this backwash bore is less pronounced compared to that in Zhu et al. (2012). This is because a much smaller  $\sigma$  value is used and bed shear stress is considered in this simulation. As in the solitary wave swash event (Zhu and Dodd, 2015), the backwash bore disappears as the backwash flow gradually slows down and changes its direction. From the backwash bore path in figure 4, we can see the backwash bore develops slightly further seawards when  $k$  increases. The bore paths are, however, very close.

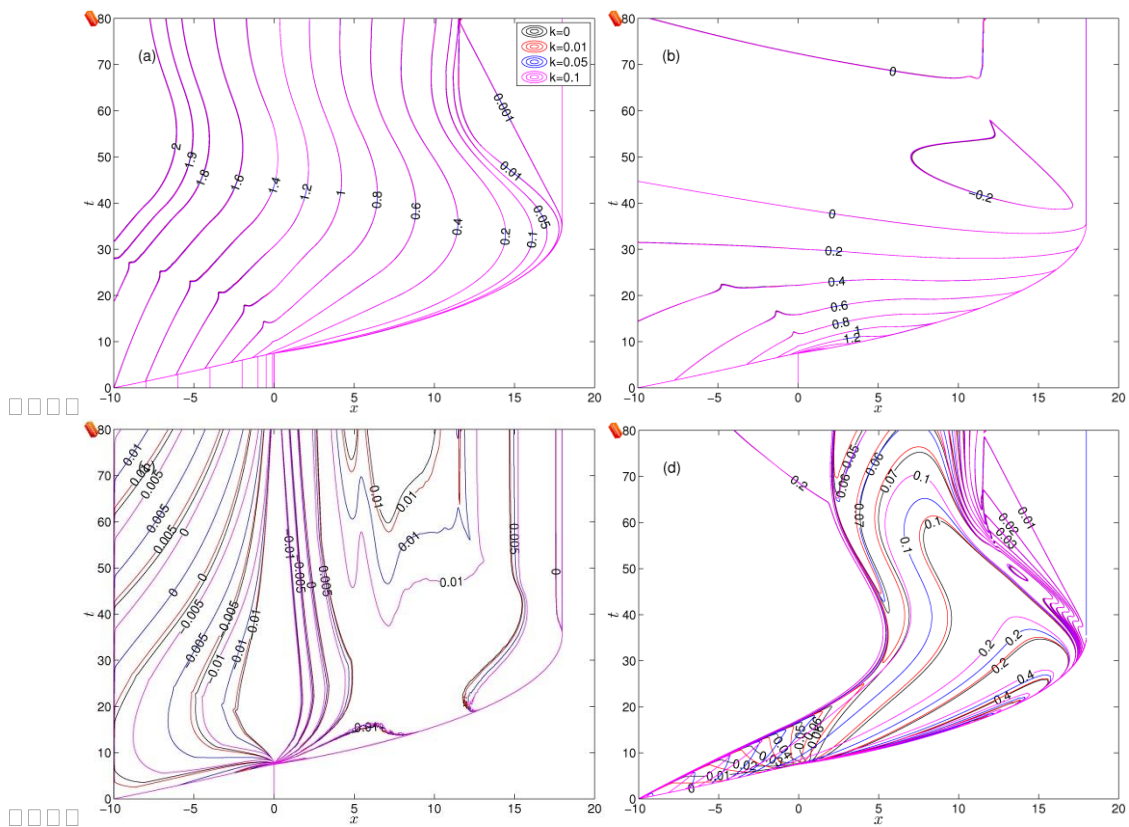


Figure 3. The mobile bed HP79 event ( $\sigma = 0.01$ ,  $M = 0.001$ ,  $\tilde{E} = 0.01$ ,  $c_d = 0.01$ ). (a)  $h$ ; (b)  $u$ ; (c) change in bed elevation,  $\Delta B = B(x, t) - B(x, t = 0)$ ; (d)  $c$ .

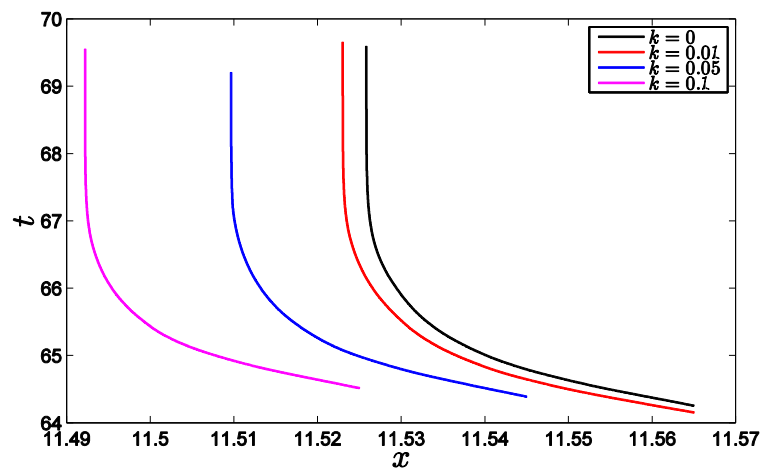


Figure 4. The backwash bore path for simulations with various  $k$  values.

We can see clearly from figure 3 (c) and (d) that the pattern of contour plots of suspended sediment concentration  $c$  and bed change  $\Delta B$  varies for different  $k$  values. When  $k$  increases, the suspended sediment concentration is larger and there is more erosion in the lower swash as the uniform bore approaches the beach. There is more deposition in the upper swash and also larger sediment concentration. With a larger  $k$  value, more sediment is suspended by the incoming bore, and it is transported to the upper swash, and deposited. This is consistent with the finding of Pritchard and Hogg (2005) that pre-suspended sediment contributes to the deposition in the upper swash. This illustrates the effect of bore turbulence, and the effects become more significant as  $k$  increases.

However, figure 3 (a) and (b) show that the inclusion of sediment entrainment due to bore turbulence has little effect on the water depth and velocity. It is consistent with the finding of Zhu and Dodd (2015) that suspended sediment has little effect on the swash hydrodynamics.

Figures 5 and 6 show more closely the bed change and sediment concentration as time varies. When  $t = 10$ , there is a decrease in bed level in the region  $-10 < x < 0$  as  $k$  increases, where the uniform bore travels (figure 5 (a)). The bed change in the region  $x > 0$  is barely noticeable. However, we can see high suspended concentration  $c$  values in the  $x > 0$  region (figure 6 (a)). We start to see the increase in bed change at  $t = 20$  (figure 5 (b)) because of the high suspended sediment concentration at earlier times (figure 6 (a)). The suspended sediment concentration decreases as sediment settles down (figure 6 (a)-(b)). Sediment continues to settle (figure 6 (b)-(d)), and consequently, the larger deposition in the  $x > 0$  region is more pronounced as time increases (figure 5 (b)-(e)).

In the backwash, there is no large increase in the suspended sediment concentration because of the slower water velocity and therefore reduced sediment entrainment. At  $t = 60$ , we can see the development of a bed step due to the backwash bore, and it further develops. We can see the sediment concentration at the backwash bore is increased (figure 6(h)). However, this increase is much smaller than that of the incoming bore. This is because the strength of this backwash bore is much smaller than that of the incoming uniform bore. Furthermore, this increase is very confined to the backwash bore, as the flow is slow and thin, and sediment advection is weak. Therefore the difference in bed change due to bore turbulence is very localised and not so significant. The bore turbulence has greater effect in the lower swash than in the upper swash. This is because the strength of the incoming bore is much larger than that of the backwash bore.

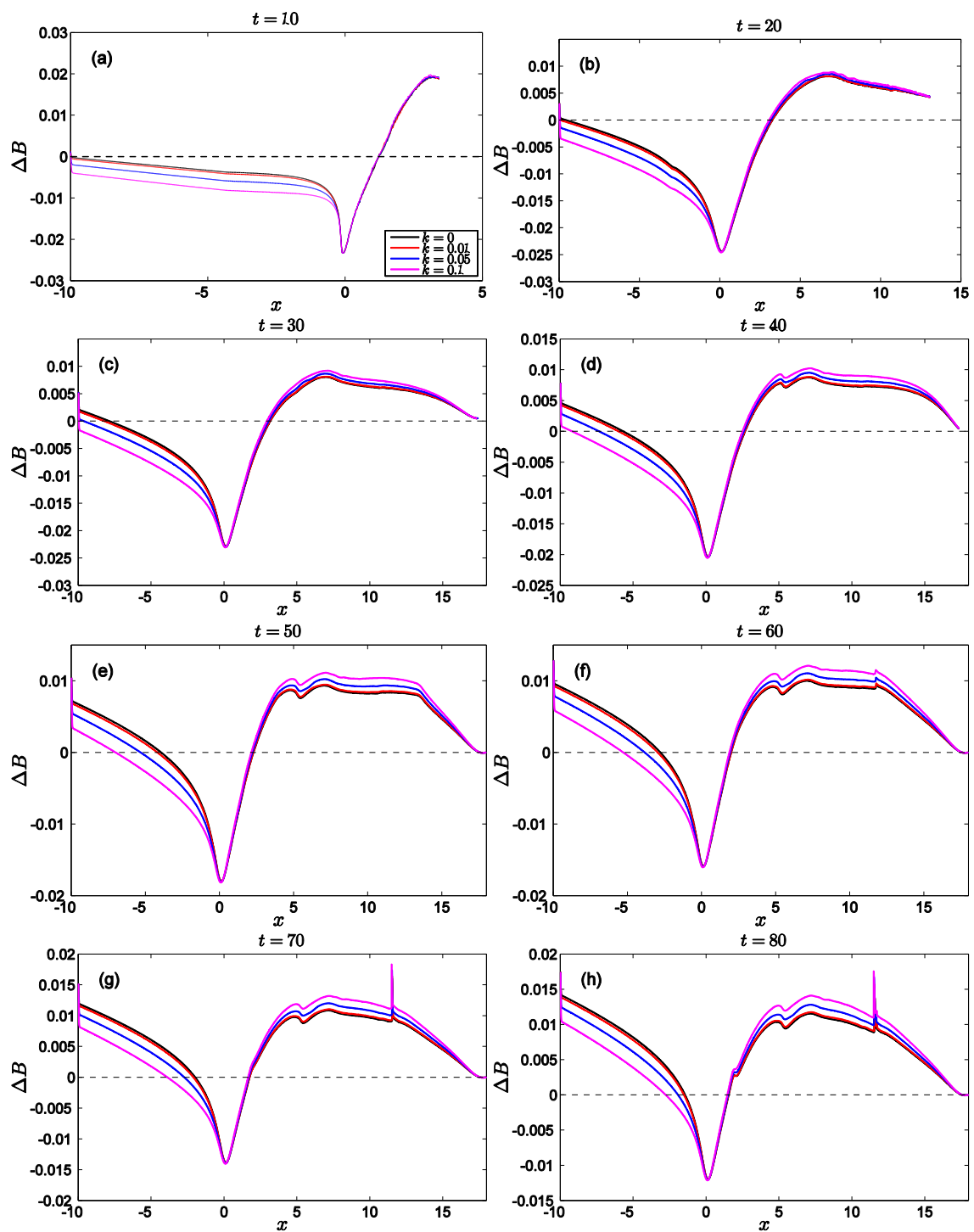


Figure 5. Beach changes  $\Delta B$  at different time series.

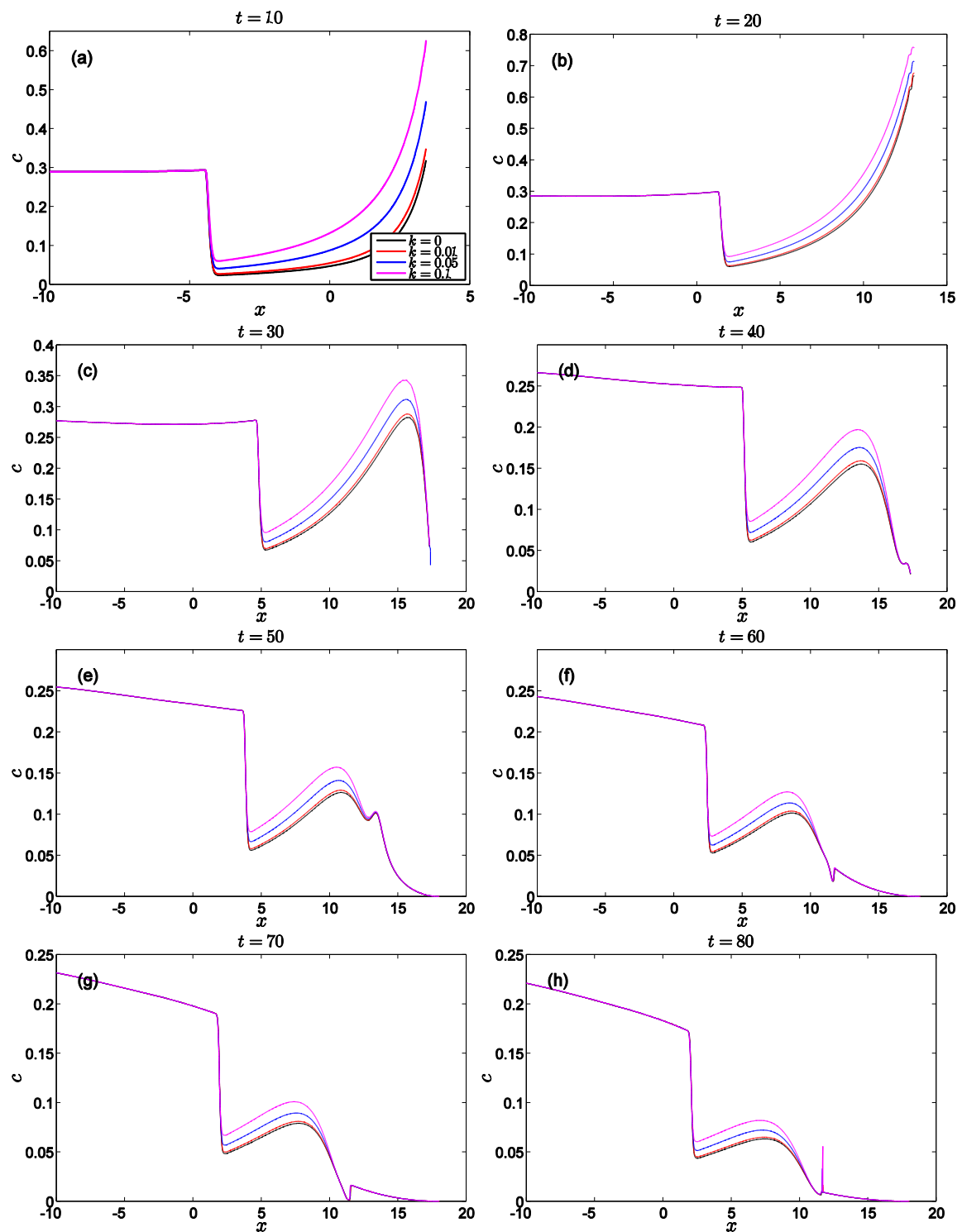


Figure 6. Suspended sediment concentration  $c$  at different time series.

### 3.3. Incoming uniform bore

We further examine the bed evolution and sediment suspension across the incoming uniform bore. Figure 7 shows the comparison of bed changes and suspended sediment concentrations on the left and right side of the bore. It should be noted that there is no bed change on the right side of the bore and there is no

suspended sediment. On the left side, there is a bed step for  $k = 0$ , and the bed change is a positive value. However, when  $k$  increases, sediment is entrained and there is much more erosion on the left side. We can see from figure 8 that the bed discontinuity associated with the incoming bore changes its direction from shoreward to seaward when  $k = 0.05$  and  $k = 0.1$ . Consequently, there is a large sediment concentration on the left side (figure 7(b)).

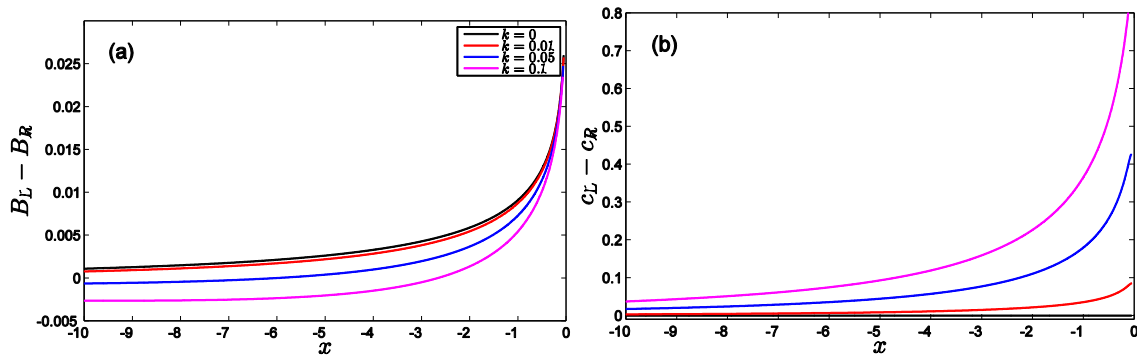


Figure 7. Bed difference (a) and suspended sediment concentration different (b) across the incoming bore at different positions.

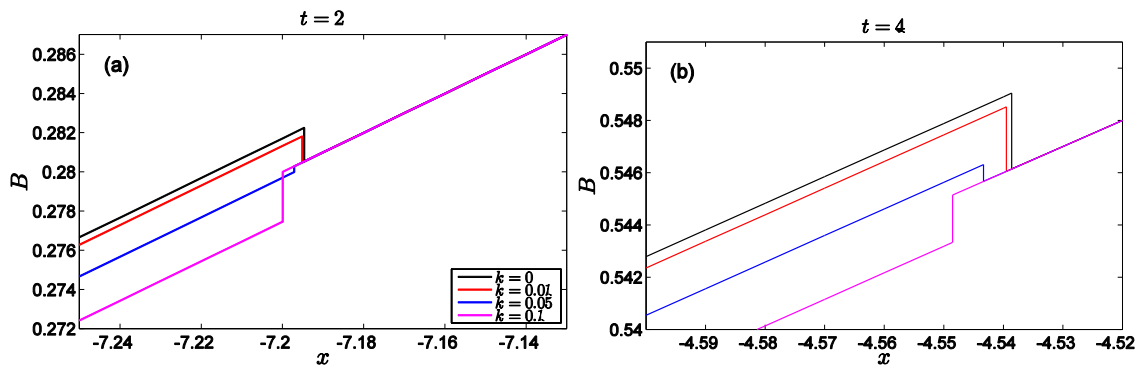


Figure 8. Bed step at the incoming bore.

### 3.4. Backwash bore

The bed steps when the backwash bores become stationary are shown in figure 9. The bed step size  $B_R - B_L$  and difference in concentration across the backwash bore at different positions are shown in figure 10. The bed step is further seawards for a larger  $k$  value. The sizes of the bed step are generally very close. The sediment concentration on the left side is larger than that on the right side although the velocity is higher on the right side. This is because the entrainment due to bore turbulence travels to the left side. The difference increases as the bore develops, and gradually decreases when the backwash bore strength is smaller. When the backwash bore becomes static there is no difference in the sediment concentration. The sediment concentration is greatly increased when  $k$  is increased to 0.1.

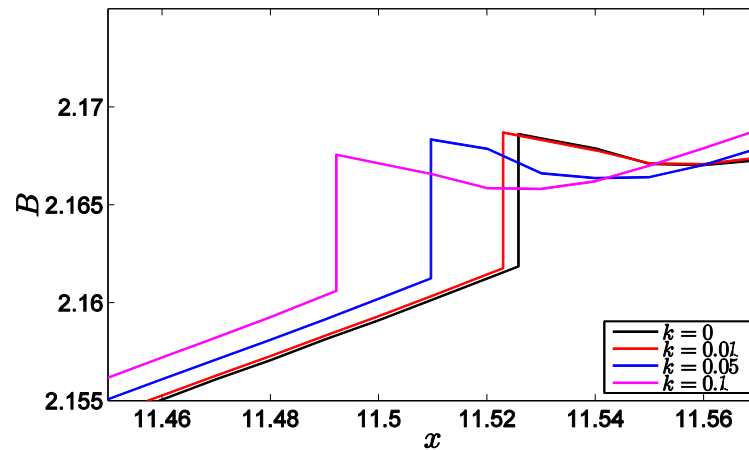


Figure 9. Bed steps when the backwash bores become stationary.

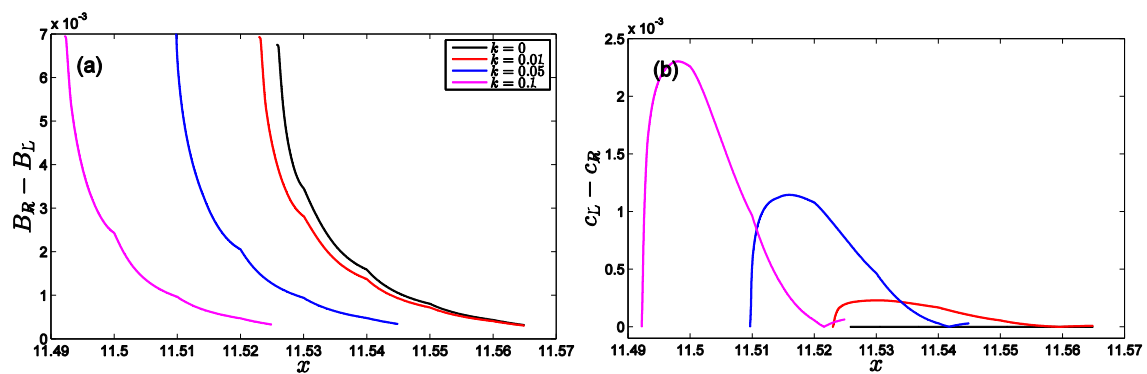


Figure 10. Bed difference (a) and suspended sediment concentration different (b) across the backwash bore at different positions.

#### 4. Conclusions

This work has proposed a new approach of estimating the bore turbulence; bore turbulence is assumed to be proportional to the energy loss at the bore. Furthermore, a single HP79 swash event has been simulated, and the beach change and sediment concentration for different  $k$  values are presented. The results show that bore generated turbulence enhances the suspension of sediment in the uprush, which is transported to the uprush and is deposited. This contributes to the relatively more deposition in the uprush. The turbulence of the backwash bore is much smaller than the incoming bore, and has less significant effects on the bed change.

#### Acknowledgements

FZ and ND would like to acknowledge the financial support from National Natural Science Foundation of China (NSFC, 51509135).

#### References

- Alsina, J. M., Falchetti, S. and Baldock, T. E., 2009. Measurements and modelling of the advection of suspended sediment in the swash zone by solitary waves. *Coastal Eng.* 56, 621-631.
- Butt, T., Russell, P., Puleo, J., Miles, J. and Masselink, G., 2004. The influence of bore turbulence on sediment transport in swash and inner surf zones. *Cont. Shelf Res.* 24, 757-771.
- Hibberd, S. and Peregrine, D. H., 1979. Surf and run-up on a beach: a uniform bore. *J. Fluid Mech.* 95, 323-345.

- Jackson, N. L., Masselink, G. and Nordstrom, K. F., 2004. The role of bore collapse and local shear stresses on the spatial distribution of sediment load in the uprush of an intermediate-state beach. *Marine Geology* 203, 109-118.
- Kelly, D. M. and DODD, N., 2010. Beach face evolution in the swash zone. *J. Fluid Mech.* 661, 316-340.
- Kobayashi, N. and Johnson, B. D., 2001. Sand suspension, storage, advection and settling in surf and swash zones. *J. Geophys. Res.* 106(C5), 9363-9376.
- Pritchard, D. and Hogg, A. J. 2005. On the transport of suspended sediment by a swash event on a plane beach. *Coast. Eng.* 52, 1-23.
- Stoker, J.J., 1957. *Water Waves*. New York, N.Y.: Interscience.
- Zhu, F. and Dodd, N., 2015. The morphodynamics of a swash event on an erodible beach. *J. Fluid Mech.* 95, 323-345.
- Zhu, F., Dodd, N. and Briganti, R. 2012. Impact of a uniform bore on an erodible beach. *Coast. Eng.* 60, 326-333.
- Zhu, F., 2012. *1D morphodynamical modelling of swash zone beachface evolution*. PhD thesis. University of Nottingham.
- Zhu, F. and Dodd, N., 2013. Net beach change in the swash: A numerical investigation. *Adv. Water Resour.* 53, 12-22.